Advances in Water Resources 32 (2009) 120–126

Contents lists available at ScienceDirect

Advances in Water Resources

journal homepage: www.elsevier.com/locate/advwatres

Stochastic analysis of bounded unsaturated flow in heterogeneous aquifers: Spectral/perturbation approach

Ching-Min Chang, Hund-Der Yeh *

Institute of Environmental Engineering, National Chiao Tung University, No. 75, Po-Ai Street, Hsinchu 300, Taiwan

ARTICLE INFO

Article history:
Received 26 May 2008
Received in revised form 14 August 2008
Accepted 21 October 2008
Available online 26 October 2008

Keywords:
Stochastic analysis
Bounded unsaturated flow
Heterogeneous media
Spectral perturbation approach

ABSTRACT

This paper describes a stochastic analysis of steady state flow in a bounded, partially saturated heterogeneous porous medium subject to distributed infiltration. The presence of boundary conditions leads to non-uniformity in the mean unsaturated flow, which in turn causes non-stationarity in the statistics of velocity fields. Motivated by this, our aim is to investigate the impact of boundary conditions on the behavior of field-scale unsaturated flow. Within the framework of spectral theory based on Fourier–Stieltjes representations for the perturbed quantities, the general expressions for the pressure head variance, variance of log unsaturated hydraulic conductivity and variance of the specific discharge are presented in the wave number domain. Closed-form expressions are developed for the simplified case of statistical isotropy of the log hydraulic conductivity field with a constant soil pore-size distribution parameter. These expressions allow us to investigate the impact of the boundary conditions, namely the vertical infiltration from the soil surface and a prescribed pressure head at a certain depth below the soil surface. It is found that the boundary conditions are critical in predicting uncertainty in bounded unsaturated flow. Our analytical expression for the pressure head variance in a one-dimensional, heterogeneous flow domain, developed using a nonstationary spectral representation approach [Li S-G, McLaughlin D. A nonstationary spectral method for solving stochastic groundwater problems: unconditional analysis. Water Resour Res 1991;27(7):1589–605; Li S-G, McLaughlin D. Using the nonstationary spectral method to analyze flow through heterogeneous trending media. Water Resour Res 1995; 31(3):541–51], is precisely equivalent to the published result of Lu et al. [Lu Z, Zhang D. Analytical solutions to steady state unsaturated flow in layered, randomly heterogeneous soils via Kirchhoff transformation. Adv Water Resour 2004;27:775–84].

1. Introduction

The field-scale behavior of unsaturated flow in unbounded heterogeneous formations has been investigated stochastically in numerous studies [8,15,16,21]. Common to these investigations is the assumption of a constant mean head gradient in the treatment of unbounded flow problem. However, in cases of bounded flow domain, a recharge from the surface may cause non-uniformity in the mean flow and consequently, non-stationarity in the statistics of random velocity fields. In the presence of a shallow water table, the constant mean gradient region may constitute only a small portion of the flow domain [9]. Therefore, the applicability of solutions developed based on a constant mean head gradient assumption to the case of bounded flow domain is excluded. Motivated by the above, this study is devoted to the quantification of the flow perturbation caused by non-uniformity of the mean unsaturated flow resulting from the imposed boundary conditions. The resulting expressions provide a basic framework for understanding and quantifying field-scale unsaturated flow processes in heterogeneous media.

The infinite-domain spectral approach [1,7,21] is appropriate in the situation where the flow domain is large compared to the correlations scale of hydraulic conductivity field; however, this spectral approach will not provide accurate predictions of the field-scale behavior of groundwater movement in cases of bounded flow domain where the boundaries introduce the non-stationarity in the statistics of random velocity fields. Li and McLaughlin [10] suggested that the infinite-domain Fourier–Stieltjes representations can be adjusted to incorporate nonstationary effects by using a transfer function, found by solving a linearized partial differential equation. This nonstationary spectral approach has proven useful in analysis of field-scale stochastic flow with a mean head gradient changing rapidly over space [3,4,11,12].

Many studies have been devoted to the modeling bounded unsaturated flow [5,9,13,14,20,22]. However, the application of the nonstationary spectral representation approach [10,11] to the

* Corresponding author. Fax: +886 35 726050.
E-mail addresses: changcm@mail.nctu.edu.tw (C.-M. Chang), hdyeh@mail.nctu.edu.tw (H.-D. Yeh).

0309-1708/$ - see front matter © 2008 Elsevier Ltd. All rights reserved.
doi:10.1016/j.advwatres.2008.10.011

investigation of the behavior of field-scale three-dimensional (3-D) unsaturated flow in a bounded domain has so far not been attempted, and this is the task undertaken here. This approach leads to develop closed-form expressions for the pressure head variance, variance of log unsaturated hydraulic conductivity and variance of the specific discharge in a bounded flow domain, which, to the best of our knowledge, have never before been presented for the 3-D unsaturated flow case.

Recharge as a major hydrology component plays an important role in regional hydrology and environment, as well as in water table change. A better knowledge of the impact of recharge on the behavior of unsaturated flow would allow an improved groundwater management and assessment of surface-applied pollution. Therefore, our investigation focuses on the impact of the boundary conditions, namely the vertical infiltration from the soil surface and a prescribed pressure head at a certain depth below the soil surface, on these results. We hope that our predictive model will improve the understanding of the impact of the boundary conditions on field-scale unsaturated flow and solute transport.

2. Unsaturated flow analysis

2.1. Statement of the problem

We are concerned with steady state flow in a partially saturated heterogeneous porous medium, where the flow domain is in a formation of infinite horizontal extent, bounded above by a constant flux at the soil surface and below by a prescribed pressure head at a certain depth below the surface. The formation properties, namely the log saturated hydraulic conductivity ($\ln K_s$) and the log soil pore-size distribution parameter ($\ln \alpha$), are modeled as random space functions with stationary means and presumed covariance structure. It is also assumed that the effect of variability of the soil moisture content is secondary relative to the effect of variability of the saturated hydraulic conductivity.

It is well known that spatial variability of soil properties affects the field-scale movement of groundwater in aquifers. The aim of the stochastic approach, therefore, is to realistically incorporate the impact of the spatial variability of soil properties into predictive models. This can be achieved by representing the local hydraulic properties in the form of statistically homogeneous random fields in 3-D space. Under this assumption, spectral techniques in conjunction with perturbation theory lead to closed-form expressions describing the statistical behavior of heterogeneous groundwater flow systems. The analysis is simplified to the case where the mean flow is aligned in the vertical direction (X_1) as the only nonzero component of the mean hydraulic gradient [19,22] but perturbations to the flow in three dimensions.

The starting point of this study is to use stochastic analysis to develop the head perturbation equation, linearized by Kirchhoff transformation, whose solution is used to determine the variability of key output processes.

The general equation describing the steady state moisture movement in a partially saturated, isotropic medium at the local scale takes the form [2]

$$\frac{\partial}{\partial X_i}\left[K(\phi)\frac{\partial \phi}{\partial X_i}\right]+\frac{\partial K(\phi)}{\partial X_1}=0, \tag{1}$$

where ϕ is the water pressure head, X_1 denotes the vertical axis and is positive pointing upward, and $K(\phi)$ is the unsaturated hydraulic conductivity, which may be decomposed as

$$K(\phi)=K_s\cdot K_r(\phi), \tag{2}$$

where K_s is the saturated hydraulic conductivity and $Kr(\phi)$ denotes the relative hydraulic conductivity. The fluid pressure is prescribed at $X_1 = X_0$

$$\phi|_{X_1=X_0}=\phi_0 \tag{3}$$

and a constant flux q_0 occurs at the soil surface ($X_1 = X_L$)

$$K_sK_r(\phi)\left(\frac{\partial \phi}{\partial X_1}+1\right)\Big|_{X_1=X_L}=-q_0. \tag{4}$$

The unsaturated flow equation (1) can be linearized with the Kirchhoff transform [13,20]

$$\varepsilon(X)=\int_{-\infty}^{\phi(X)}K_r(S)dS. \tag{5}$$

With the aid of the identities

$$\frac{\partial \varepsilon}{\partial X_i}=\frac{\partial \varepsilon}{\partial \phi}\frac{\partial \phi}{\partial X_i}=K_r(\phi)\frac{\partial \phi}{\partial X_i} \tag{6}$$

and

$$\frac{\partial K_r}{\partial X_1}=\frac{\partial K_r}{\partial \phi}\frac{1}{\frac{\partial \varepsilon}{\partial \phi}}\frac{\partial \varepsilon}{\partial X_1}=\frac{1}{K_r}\frac{\partial K_r}{\partial \phi}\frac{\partial \varepsilon}{\partial X_1}. \tag{7}$$

Eq. (1) leads to

$$\frac{\partial^2 \varepsilon}{\partial X_i^2}+\frac{\partial \ln K_s}{\partial X_i}\frac{\partial \varepsilon}{\partial X_i}+\frac{1}{K_r}\frac{\partial K_r}{\partial \phi}\frac{\partial \varepsilon}{\partial X_1}+K_r\frac{\partial \ln K_s}{\partial X_1}=0. \tag{8}$$

Assume that the relative hydraulic conductivity at the local level is related to the pressure head by Gardner [6]

$$K_r(X,\phi)=\exp[\alpha(X)\phi], \tag{9}$$

where α is a soil pore-size distribution parameter. The exponential hydraulic conductivity model has been used widely to simplify the task of solving the unsaturated flow equation [13,14,17,18,20,21]. Introducing Eq. (9) into Eq. (5) results in

$$\varepsilon(\boldsymbol{X})=\frac{1}{\alpha}\exp[\alpha(\boldsymbol{X})\phi]=\frac{K_r}{\alpha}. \tag{10}$$

Substituting Eqs. (9) and (10) into Eq. (8) gives a linear partial differential equation

$$\frac{\partial^2 \varepsilon}{\partial X_i^2}+\frac{\partial \ln K_s}{\partial X_i}\frac{\partial \varepsilon}{\partial X_i}+\alpha\frac{\partial \varepsilon}{\partial X_1}+\alpha\frac{\partial \ln K_s}{\partial X_1}\varepsilon=0. \tag{11}$$

By virtue of Eqs. (5) and (9), the boundary conditions Eqs. (3) and (4) are expressed in the forms, respectively, as

$$\varepsilon|_{X_1=X_0}=\frac{e^{\alpha\phi_0}}{\alpha}, \tag{12a}$$

$$\left(\frac{\partial \varepsilon}{\partial X_1}+\alpha\varepsilon\right)\Big|_{X_1=X_L}=-\frac{q_0}{K_s}. \tag{12b}$$

2.2. Pressure head perturbation

In the analysis that follows, $\ln K_s$, $\ln \alpha$ and ε are considered to be random space functions and decomposed into ensemble means and small perturbations around the mean

$$\begin{aligned}\ln K_s&=\langle \ln K_s\rangle+f=F+f,\\ \ln\alpha&=\langle\ln\alpha\rangle+\beta=B+\beta,\\ \varepsilon&=\langle\varepsilon\rangle+\varepsilon'=\bar{\varepsilon}+\varepsilon',\end{aligned} \tag{13}$$

where $\langle\rangle$ stands for the ensemble average. Substituting the perturbed forms given in Eq. (13) into Eqs. (11), (12a) and (12b), expanding terms and taking the mean produces the following mean equation, approximated to the first-order in perturbation products:

$$\frac{\partial^2 \bar{\varepsilon}}{\partial X_i^2}+\alpha_g\frac{\partial \bar{\varepsilon}}{\partial X_1}=0 \tag{14}$$

subject to the boundary conditions

$$\bar{\varepsilon}(X_0) = \frac{\exp[\alpha_g \phi_0]}{\alpha_g}, \tag{15a}$$

$$\left(\frac{\partial \bar{\varepsilon}}{\partial X_1} + \alpha_g \bar{\varepsilon}\right)\bigg|_{X_1 = X_L} = -\frac{q_0}{K_g}, \tag{15b}$$

where $\alpha_g = \exp(B)$ and $K_g = \exp[F]$. The detailed development of Eq. (15a) was given by Lu and Zhang [13]. It follows from Eq. (13) that $K_s = \exp(F + f)$ and $\alpha = \exp(B + \beta)$. Substituting them into Eq. (12a), expanding $\exp(-f)$ and $\exp(\beta)$ in terms of power series, retaining terms up to the fist-order and taking the mean leads to Eq. (15b).

The first-order perturbation approximation is developed by subtracting the mean equation from the perturbation representation of Eq. (11) and neglecting products of perturbation quantities beyond the second-order

$$\frac{\partial^2 \varepsilon'}{\partial X_i^2} + \alpha_g \frac{\partial \varepsilon'}{\partial X_1} + \left[\frac{\partial \bar{\varepsilon}}{\partial X_i}\frac{\partial f}{\partial X_i} + \alpha_g \bar{\varepsilon}\frac{\partial f}{\partial X_1}\right] + \alpha_g \beta \frac{\partial \bar{\varepsilon}}{\partial X_1} = 0 \tag{16}$$

subject to the boundary conditions

$$\varepsilon'(X_0) = \frac{\exp[\alpha_g \phi_0]}{\alpha_g}(\alpha_g \phi_0 - 1)\beta, \tag{17a}$$

$$\left(\frac{\partial \varepsilon'}{\partial X_1} + \alpha_g \varepsilon' + \alpha_g \bar{\varepsilon}\beta\right)\bigg|_{X_1 = X_L} = \frac{q_0}{K_g} f. \tag{17b}$$

It follows from Eqs. (14) and (16) that the imposed boundary conditions produce a space-dependent $\bar{\varepsilon}$, and consequently, results in a nonstationary solution, ε', to Eq. (16).

The approach followed is to develop the solution to the perturbation equation in order to quantify the variability of pressure head. Under the unidirectional mean flow condition, Eq. (16) can be simplified to

$$\frac{\partial^2 \varepsilon'}{\partial X_i^2} + \alpha_g \frac{\partial \varepsilon'}{\partial X_1} + \left[\frac{\partial \bar{\varepsilon}}{\partial X_1} + \alpha_g \bar{\varepsilon}\right]\frac{\partial f}{\partial X_1} + \alpha_g \beta \frac{\partial \bar{\varepsilon}}{\partial X_1} = 0. \tag{18}$$

To solve Eq. (18), one needs to know the spatial behavior of $\bar{\varepsilon}$ and its space gradient, which in turn, requires solving the mean flow equation (14).

In the case of unidirectional mean flow, the corresponding solution to Eq. (14), subject to the boundary conditions (15a) and (15b), is given by [13,14]

$$\bar{\varepsilon}(X_1) = \frac{\exp[\alpha_g(\phi_0 - (X_1 - X_0))]}{\alpha_g} + \frac{q_0}{\alpha_g K_g}[\exp[-\alpha_g(X_1 - X_0)] - 1]. \tag{19}$$

Substitution of Eq. (19) and its space gradient into Eq. (18) yields

$$\frac{\partial^2 \varepsilon'}{\partial X_i^2} + \alpha_g \frac{\partial \varepsilon'}{\partial X_1} = \frac{q_0}{K_g}\frac{\partial f}{\partial X_1} + \alpha_g \gamma(X_1)\beta, \tag{20}$$

where

$$\gamma(X_1) = \exp[\alpha_g[\phi_0 - (X_1 - X_0)]] + (q_0/K_g)\exp[-\alpha_g(X_1 - X_0)]. \tag{21}$$

Eq. (20) can be solved using the nonstationary spectral representation [10,11] based on Fourier–Stieltjes representation for the perturbed quantities in wave number domain. By using this approach, the random perturbations are represented by the following 3-D wave number integrals:

$$f(\boldsymbol{X}) = \int_{-\infty}^{\infty} \exp[i\boldsymbol{R}\cdot\boldsymbol{X}]dZ_f(\boldsymbol{R}), \tag{22}$$

$$\beta(\boldsymbol{X}) = \int_{-\infty}^{\infty} \exp[i\boldsymbol{R}\cdot\boldsymbol{X}]dZ_\beta(\boldsymbol{R}), \tag{23}$$

$$\varepsilon'(\boldsymbol{X}) = \int_{-\infty}^{\infty} \Phi_f(\boldsymbol{X},\boldsymbol{R})dZ_f(\boldsymbol{R}) + \int_{-\infty}^{\infty} \Phi_\beta(\boldsymbol{X},\boldsymbol{R})dZ_\beta(\boldsymbol{R}), \tag{24}$$

where $\Phi_f(\boldsymbol{X},\boldsymbol{R})$ and $\Phi_\beta(\boldsymbol{X},\boldsymbol{R})$ are transfer functions to be given, $dZ_f(\boldsymbol{R})$ is the complex Fourier amplitude of $\ln K_s$, $dZ_\beta(\boldsymbol{R})$ is the complex Fourier amplitude of $\ln\alpha$ and $\boldsymbol{R} = (K_1, K_2, K_3)$ is the wave number vector. Note that Eq. (24) is represented based on the principle of superposition, which is applicable to any linear system, including algebraic equations and linear differential equations. The first term on the right-hand side of Eq. (24) reflects the effect of the variation of the log hydraulic conductivity, while the second term reflects the effect of the variation of the log soil pore-size distribution parameter.

By applying the superposition principle, the linear differential equation (20) can be divided into two sub-equations: one describing the response of the log hydraulic conductivity variation and the other the variation of soil pore-size distribution parameter. The results of each part is summed to obtain the solution to the original problem. Using Eqs. (22)–(24) in Eq. (20) and uniqueness of the representations results in two sub-equations

$$\frac{\partial^2 \Phi_f}{\partial X_i^2} + \alpha_g \frac{\partial \Phi_f}{\partial X_1} = i\frac{q_0}{K_g}R_1 \exp[i\boldsymbol{R}\cdot\boldsymbol{X}], \tag{25}$$

$$\frac{\partial^2 \Phi_\beta}{\partial X_i^2} + \alpha_g \frac{\partial \Phi_\beta}{\partial X_1} = \alpha_g \gamma(X_1)\exp[i\boldsymbol{R}\cdot\boldsymbol{X}]. \tag{26}$$

The solutions to Eqs. (25) and (26) give the transfer functions

$$\Phi_f = -i\frac{q_0}{K_g}\frac{R_1}{R^2 - i\alpha_g R_1}\exp[i\boldsymbol{R}\cdot\boldsymbol{X}], \tag{27}$$

$$\Phi_\beta = -\alpha_g \gamma(X_1)\frac{1}{R^2 + i\alpha_g R_1}\exp[i\boldsymbol{R}\cdot\boldsymbol{X}]. \tag{28}$$

To take the advantage of a closed-form expression, the boundary effects on the head fluctuation is assumed negligible [3,4,11,12] in obtaining solutions to Eqs. (25) and (26). It is expected the boundary effect is largely limited to a small zone next to the medium boundary.

In terms of the above transfer functions of Φ_f and Φ_β, Eq. (24) can be written as

$$\varepsilon'(\boldsymbol{X}) = -\frac{q_0}{K_g}\int_{-\infty}^{\infty}\frac{iR_1}{R^2 - i\alpha_g R_1}\exp[i\boldsymbol{R}\cdot\boldsymbol{X}]dZ_f(\boldsymbol{R}) - \alpha_g\gamma(X_1) \times \int_{-\infty}^{\infty}\frac{1}{R^2 + i\alpha_g R_1}\exp[i\boldsymbol{R}\cdot\boldsymbol{X}]dZ_\beta(\boldsymbol{R}). \tag{29}$$

2.3. Variances of pressure head and log unsaturated hydraulic conductivity

Following Tartakovsky et al. [20] and Lu and Zhang [13], we note from Eqs. (9) and (10) that the variance of pressure head σ_ϕ^2 can be expressed as

$$\sigma_\phi^2 = \left(\frac{1 - \alpha_g\bar{\phi}}{\alpha_g}\right)^2 \sigma_\beta^2 + 2\frac{1 - \alpha_g\bar{\phi}}{\alpha_g^2}\langle\varepsilon'\beta\rangle + \frac{\sigma_\varepsilon^2}{\alpha_g^2\bar{\varepsilon}^2}, \tag{30}$$

where σ_ε^2 is the variance of ε, σ_β^2 is the variance of $\ln\alpha$ and $\bar{\phi} = \ln[\alpha_g\bar{\varepsilon}]/\alpha_g$. Using the representation theorem for ε', it follows that

$$\langle\varepsilon'\beta\rangle = \frac{q_0}{K_g}\alpha_g\int_{-\infty}^{\infty}\frac{R_1^2}{R^4 + \alpha_g^2 R_1^2}S_{\beta f}(\boldsymbol{R})d\boldsymbol{R} - \alpha_g\gamma(X_1)\int_{-\infty}^{\infty}\frac{R^2}{R^4 + \alpha_g^2 R_1^2}S_{\beta\beta}(\boldsymbol{R})d\boldsymbol{R} \tag{31}$$

and

$$\sigma_\varepsilon^2 = \left(\frac{q_0}{K_g}\right)^2\int_{-\infty}^{\infty}\frac{R_1^2}{R^4 + \alpha_g^2 R_1^2}S_{ff}(\boldsymbol{R})d\boldsymbol{R} - 4\alpha_g^2\gamma(X_1)\int_{-\infty}^{\infty}\frac{R^2 R_1^2}{(R^4 + \alpha_g^2 R_1^2)^2}S_{\beta f}(\boldsymbol{R})d\boldsymbol{R} + \alpha_g^2\gamma^2(X_1)\int_{-\infty}^{\infty}\frac{1}{R^4 + \alpha_g^2 R_1^2}S_{\beta\beta}(\boldsymbol{R})d\boldsymbol{R}, \tag{32}$$

where $S_{ff}(\boldsymbol{R})$ is the spectrum of $\ln K_s$, $S_{\beta f}(\boldsymbol{R})$ is the cross-spectral spectra of the β and f processes and $S_{\beta\beta}(\boldsymbol{R})$ is the spectrum of $\ln\alpha$.

As in Yeh et al. [21], the expansion of (9) in Taylor series, ignoring the product of perturbations and application of the expectation operator to Eqs. (2) and (9) leads to the corresponding perturbation of $\ln K$, $\ln K - \langle \ln K\rangle = \alpha_g\bar{\phi}\beta + \alpha_g\phi' + f$, where ϕ' is the perturbation of pressure head and related to ε', according to Lu and Zhang [12], by $\phi' = (1-\alpha_g\bar{\phi})\beta/\alpha_g + \varepsilon'/(\bar{\varepsilon}\alpha_g)$. As such, the variance of log unsaturated hydraulic conductivity then can be expressed as

$$\sigma^2_{\ln K} = \sigma^2_\beta + 2\langle\beta f\rangle + \frac{2}{\bar{\varepsilon}}\langle\varepsilon'\beta\rangle + \frac{\sigma^2_\varepsilon}{\bar{\varepsilon}^2} + \frac{2}{\bar{\varepsilon}}\langle\varepsilon' f\rangle + \sigma^2_f, \tag{33}$$

where $\langle\beta f\rangle$ is the integration of the cross-spectral spectra of β and f, $\langle\varepsilon'\beta\rangle$ is given by (31) and

$$\langle\varepsilon' f\rangle = \left(\frac{q_0}{K_g}\right)\alpha_g\int_{-\infty}^{\infty}\frac{R_1^2}{R^4+\alpha_g^2R_1^2}S_{ff}(\boldsymbol{R})d\boldsymbol{R} - \alpha_g\gamma(X_1)\int_{-\infty}^{\infty}\frac{R^2}{R^4+\alpha_g^2R_1^2}S_{\beta f}(\boldsymbol{R})d\boldsymbol{R}. \tag{34}$$

2.4. Flow perturbation

With Eq. (29), we now start to quantify the specific discharge spectrum which can be determined from the linearized first-order perturbation approximation of Darcy's law, such as those presented by Gelhar and Axness [7] and Yeh et al. [21].

Applying Eqs. (6) and (7) to Darcy's law

$$q_i = -K_s\left[K_r\frac{\partial\phi}{\partial X_i} + \delta_{i1}K_r\right] \tag{35}$$

leads to

$$q_i = -K_s\left[\frac{\partial\varepsilon}{\partial X_i} + \delta_{i1}\alpha\varepsilon\right]. \tag{36}$$

Then the corresponding equations for the mean specific discharge and perturbation to Eq. (36) take the forms

$$\overline{q_i} = -e^F\left[\frac{\partial\bar{\varepsilon}}{\partial X_i} + \delta_{i1}\alpha_g\bar{\varepsilon}\right], \tag{37}$$

$$q_i' = -e^F\left\{\frac{\partial\varepsilon'}{\partial X_i} + \delta_{i1}\left[f\frac{\partial\bar{\varepsilon}}{\partial X_1} + \alpha_g(\varepsilon' + \beta\bar{\varepsilon} + f\bar{\varepsilon})\right]\right\}. \tag{38}$$

Substituting Fourier–Stieltjes representations for the specific discharge perturbations

$$q_i' = \int_{-\infty}^{\infty}\exp[i\boldsymbol{R}\cdot\boldsymbol{X}]dZ_{q_i}(\boldsymbol{R}) \tag{39}$$

and the representations in Eq. (29) with its gradients

$$\frac{\partial\varepsilon'}{\partial X_1} = \frac{q_0}{K_g}\int_{-\infty}^{\infty}\frac{R_1^2}{R^2 - i\alpha_gR_1}\exp[i\boldsymbol{R}\cdot\boldsymbol{X}]dZ_f(\boldsymbol{R}) + \alpha_g\gamma(X_1)\int_{-\infty}^{\infty}\frac{\alpha_g - iR_1}{R^2 + i\alpha_gR_1}\exp[i\boldsymbol{R}\cdot\boldsymbol{X}]dZ_\beta(\boldsymbol{R}), \tag{40}$$

$$\frac{\partial\varepsilon'}{\partial X_2} = \frac{q_0}{K_g}\int_{-\infty}^{\infty}\frac{R_1R_2}{R^2 - i\alpha_gR_1}\exp[i\boldsymbol{R}\cdot\boldsymbol{X}]dZ_f(\boldsymbol{R}) - \alpha_g\gamma(X_1)\int_{-\infty}^{\infty}\frac{iR_2}{R^2 + i\alpha_gR_1}\exp[i\boldsymbol{R}\cdot\boldsymbol{X}]dZ_\beta(\boldsymbol{R}), \tag{41}$$

$$\frac{\partial\varepsilon'}{\partial X_3} = \frac{q_0}{K_g}\int_{-\infty}^{\infty}\frac{R_1R_3}{R^2 - i\alpha_gR_1}\exp[i\boldsymbol{R}\cdot\boldsymbol{X}]dZ_f(\boldsymbol{R}) - \alpha_g\gamma(X_1)\int_{-\infty}^{\infty}\frac{iR_3}{R^2 + i\alpha_gR_1}\exp[i\boldsymbol{R}\cdot\boldsymbol{X}]dZ_\beta(\boldsymbol{R}) \tag{42}$$

into Eq. (38) and using the uniqueness of the spectrum presentations yields

$$dZ_{q_1} = -K_g\left\{\frac{q_0}{K_g}\frac{-R^2+R_1^2}{R^2 - i\alpha_gR_1}dZ_f + \alpha_g\frac{\bar{\varepsilon}R^2 - i(q_0/K_g)R_1}{R^2 + i\alpha_gR_1}dZ_\beta\right\}, \tag{43}$$

$$dZ_{q_2} = -K_g\left\{\frac{q_0}{K_g}\frac{R_1R_2}{R^2 - i\alpha_gR_1}dZ_f - \alpha_g\frac{i\gamma(X_1)R_2}{R^2 + i\alpha_gR_1}dZ_\beta\right\}, \tag{44}$$

$$dZ_{q_3} = -K_g\left\{\frac{q_0}{K_g}\frac{R_1R_3}{R^2 - i\alpha_gR_1}dZ_f - \alpha_g\frac{i\gamma(X_1)R_3}{R^2 + i\alpha_gR_1}dZ_\beta\right\}. \tag{45}$$

Taking the expected value of the product of the Fourier amplitude and its complex conjugate gives the spectrum for the stochastic process. Thus it follows from Eqs. (43)–(45) that

$$S_{q_1q_1}(\boldsymbol{R}) = K_g^2\left\{\left(\frac{q_0}{K_g}\right)^2\frac{R^4-2R^2R_1^2+R_1^4}{R^4+\alpha_g^2R_1^2}S_{ff}(\boldsymbol{R}) + \alpha_g^2\frac{\bar{\varepsilon}^2R^4+(q_0/K_g)^2R_1^2}{R^4+\alpha_g^2R_1^2}S_{\beta\beta}(\boldsymbol{R}) + 2\alpha_g\frac{q_0}{K_g} \times\frac{\bar{\varepsilon}(-R^4+R^2R_1^2)(R^4-\alpha_g^2R_1^2)-2(q_0/K_g)\alpha_gR^2R_1^2(-R^2+R_1^2)}{(R^4+\alpha_g^2R_1^2)^2}S_{\beta f}(R)\right\}, \tag{46}$$

$$S_{q_2q_2}(\boldsymbol{R}) = K_g^2\left\{\left(\frac{q_0}{K_g}\right)^2\frac{R_1^2R_2^2}{R^4+\alpha_g^2R_1^2}S_{ff}(\boldsymbol{R}) - 4\alpha_g^2\gamma\frac{q_0}{K_g}\frac{R^2R_1^2R_2^2}{(R^4+\alpha_g^2R_1^2)^2}S_{\beta f}(\boldsymbol{R}) + \alpha_g^2\gamma^2\frac{R_2^2}{R^4+\alpha_g^2R_1^2}S_{\beta\beta}(\boldsymbol{R})\right\}, \tag{47}$$

$$S_{q_3q_3}(\boldsymbol{R}) = K_g^2\left\{\left(\frac{q_0}{K_g}\right)^2\frac{R_1^2R_3^2}{R^4+\alpha_g^2R_1^2}S_{ff}(\boldsymbol{R}) - 4\alpha_g^2\gamma\frac{q_0}{K_g}\frac{R^2R_1^2R_3^2}{(R^4+\alpha_g^2R_1^2)^2}S_{\beta f}(\boldsymbol{R}) + \alpha_g^2\gamma^2\frac{R_3^2}{R^4+\alpha_g^2R_1^2}S_{\beta\beta}(\boldsymbol{R})\right\}, \tag{48}$$

where $S_{qiqi}(\boldsymbol{R})$ is the spectrum of the specific discharge.

Integration of Eqs. (46)–(48) over the wave number domain yields the variances of the specific discharge in the longitudinal and transverse directions, respectively,

$$\sigma^2_{q_1} = K_g^2\left\{\left(\frac{q_0}{K_g}\right)^2\int_{-\infty}^{\infty}\frac{R^4-2R^2R_1^2+R_1^4}{R^4+\alpha_g^2R_1^2}S_{ff}(\boldsymbol{R})d\boldsymbol{R} + \alpha_g^2\int_{-\infty}^{\infty}\frac{\bar{\varepsilon}^2R^4+(q_0/K_g)^2R_1^2}{R^4+\alpha_g^2R_1^2}S_{\beta\beta}(\boldsymbol{R})d\boldsymbol{R} + 2\alpha_g\frac{q_0}{K_g} \times\int_{-\infty}^{\infty}\frac{\bar{\varepsilon}(-R^4+R^2R_1^2)(R^4-\alpha_g^2R_1^2)-2(q_0/K_g)\alpha_gR^2R_1^2(-R^2+R_1^2)}{(R^4+\alpha_g^2R_1^2)^2}S_{\beta f}(\boldsymbol{R})d\boldsymbol{R}\right\}, \tag{49}$$

$$\sigma^2_{q_2} = \sigma^2_{q_3} = K_g^2\left\{\left(\frac{q_0}{K_g}\right)^2\int_{-\infty}^{\infty}\frac{R_1^2R_2^2}{R^4+\alpha_g^2R_1^2}S_{ff}(\boldsymbol{R})d\boldsymbol{R} + \alpha_g^2\gamma^2(X_1) \times\int_{-\infty}^{\infty}\frac{R_2^2}{R^4+\alpha_g^2R_1^2}S_{\beta\beta}(\boldsymbol{R})d\boldsymbol{R} - 4\alpha_g^2\gamma\frac{q_0}{K_g}\int_{-\infty}^{\infty}\frac{R^2R_1^2R_2^2}{(R^4+\alpha_g^2R_1^2)^2}S_{\beta f}(\boldsymbol{R})d\boldsymbol{R}\right\}. \tag{50}$$

3. Analytical solutions: statistically isotropic media with a constant α

Eqs. (30), (33), (49) and (50) in conjunction with Eqs. (46)–(48) provide the framework required to quantify the pressure head variance, variance of log unsaturated hydraulic conductivity and variabilities of the specific discharge in the longitudinal and transverse directions, respectively, in terms of the input soil hydraulic parameters. In this section, we implement those results to the particular case of statistical isotropy of the $\ln K_s$ field with a constant α (i.e., $\alpha_g = \alpha$, $\sigma_\beta^2 = 0$, $\langle \beta f \rangle = 0$ and $\langle \varepsilon' \beta \rangle = 0$), which allows for the development of closed-form expressions.

It is assumed that the random $\ln K_s$ perturbation field f is characterized by the following spectral density function [1,7,21]:

$$S_{ff}(\boldsymbol{R}) = \frac{\sigma_f^2 \lambda^3}{\pi^2 (1 + \lambda^2 R^2)^2}, \tag{51}$$

where σ_f^2 is the variance of $\ln K_s$ and λ is the correlation scale of $\ln K_s$.

The variance of pressure head perturbation is obtained by substituting Eqs. (51) and (32) into Eq. (30) and integrating Eq. (30) over the wave domain

$$\sigma_\phi^2 = \frac{\sigma_f^2}{\alpha_g^2 \rho^2} \left(\frac{q_0}{K_g}\right)^2 \left[1 + \frac{1}{1+\mu} - \frac{2}{\mu} \ln(1+\mu)\right], \tag{52}$$

where $\mu = \alpha_g \lambda$, $\rho = \alpha_g \bar{\varepsilon} = \exp[\mu[\phi_0/\lambda - \xi]] - (q_0/K_g)(1 - \exp[-\mu\xi])$ and $\xi = (X_1 - X_0)/\lambda$. It is important to recognize from Eq. (4) that the specific flux q_0 is negative for infiltration. Clearly, in the limit of $\xi \to \infty$, ρ approaches $-q_0/K_g$ and Eq. (52) converges to the unbounded flow domain limit of the pressure head variance

$$\sigma_\phi^2 = \frac{\sigma_f^2}{\alpha_g^2} \left[1 + \frac{1}{1+\mu} - \frac{2}{\mu} \ln(1+\mu)\right], \tag{53}$$

which is equivalent to the result of Yeh et al. [21] with the assumption of unit mean head gradient.

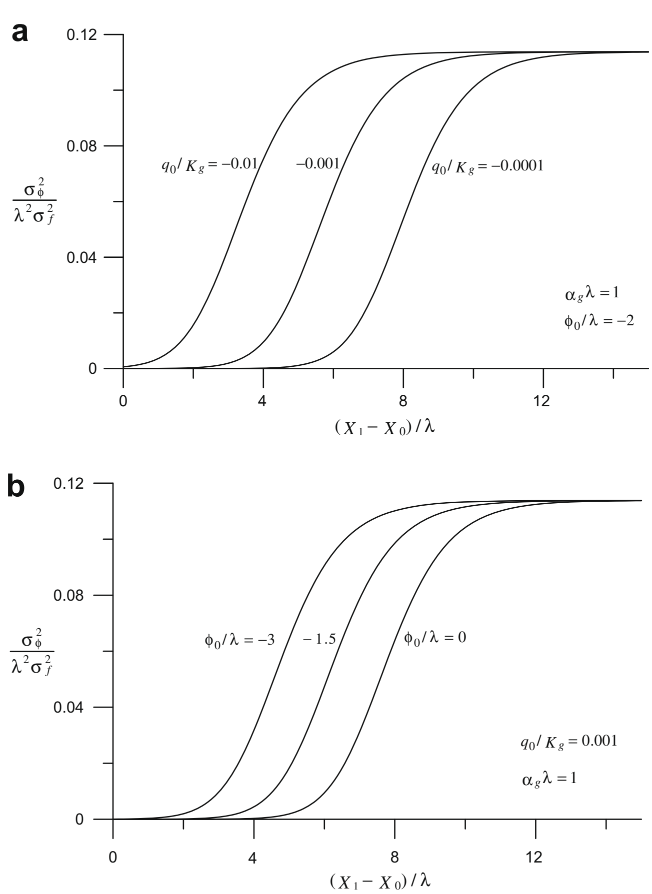

Fig. 1. Dimensionless variance of pressure head versus dimensionless distance from the boundary of constant pressure head for various (a) infiltration rates and (b) prescribed pressure heads at the bottom boundary.

Fig. 1a and b illustrates the spatial distribution of the variance of pressure head for various infiltration rates and prescribed pressure heads at the bottom boundary, respectively, based on Eq. (52). The phenomenon that the pressure head variance increases with the infiltration rate can be attributed to the influence of the pore-scale variability on the pressure head variability which is more persistent for a larger infiltration rate. The variability of the pressure head appears to be stationary toward the soil surface (a gravity-dominated region) where an unit mean hydraulic gradient has been reached. As expected, boundaries with higher prescribed pressure head (more negative) produce much higher pressure variability for a given infiltration rate. This is a consequence of the conditioning effect of the fixed pressure at the boundary. There is a transition from the gravity-dominated region to the boundary. The lower is the prescribed pressure head, the smaller is the transition; in other words, when the prescribed pressure head is low, only minor adjustments are necessary to reach the equilibrium value of pressure head, which in turn reduces the pressure head fluctuations. Substituting Eqs. (51) and (34) into Eq. (33) and integrating Eq. (33) over the wave domain results in

$$\sigma_{\ln K}^2 = \sigma_f^2 \left\{1 + \frac{1}{\rho}\frac{q_0}{K_g}\left(\frac{1}{\rho}\frac{q_0}{K_g} + 2\right)\left[1 + \frac{1}{1+\mu} - \frac{2}{\mu}\ln(1+\mu)\right]\right\} \tag{54}$$

with the corresponding limit for the unbounded flow case $\xi \to \infty$ [20]

$$\sigma_{\ln K}^2 = \sigma_f^2 \left[\frac{2}{\mu}\ln(1+\mu) - \frac{1}{1+\mu}\right]. \tag{55}$$

Fig. 2a indicates the variance of $\log K$ varying with the infiltration rate. The result agrees with our physical intuition: for a given formation properties, the smaller the infiltration rate, the dryer the soil and, consequently, the more variation in soil moisture content. Therefore, the variance of $\log K$ will increase with decreasing infiltration rate. The decrease in the variance of $\log K$ with an increase in constant pressure head at the bottom boundary is displayed in Fig. 2b. It is clear that the variance of $\log K$ is stationary along the unit gradient mean flow region.

The integral expressions in Eqs. (49) and (50) for the variances of the specific discharge in the longitudinal and transverse directions are integrated analytically using Eq. (51) to yield

$$\sigma_{q_1}^2 = \sigma_f^2 q_0^2 \left\{-\frac{5}{2}\frac{1}{\mu} + \frac{6}{\mu^2} + \frac{3}{\mu^3} - \frac{6}{\mu^4} + \ln(1+\mu)\left[\frac{2}{\mu} - \frac{8}{\mu^3} + \frac{6}{\mu^5}\right]\right\}, \tag{56}$$

$$\sigma_{q_2}^2 = \sigma_{q_3}^2 = \sigma_f^2 q_0^2 \left\{\frac{1}{4}\frac{1}{\mu} - \frac{1}{\mu^2} - \frac{3}{2}\frac{1}{\mu^3} + \frac{3}{\mu^4} + \ln(1+\mu)\left[\frac{2}{\mu^3} - \frac{3}{\mu^5}\right]\right\}. \tag{57}$$

From (30), $\bar{\phi} = \ln[\alpha_g \bar{\varepsilon}]/\alpha_g$ implies that $\bar{\varepsilon} = \exp[\alpha_g \bar{\phi}]/\alpha_g$. Recall that as $\xi \to \infty$, $\bar{\varepsilon} = -q_0/(K_g \alpha_g)$. With those, $-q_0/K_g = \exp[\alpha_g \bar{\phi}]$ (or $q_0 = -K_g \exp[\alpha_g \bar{\phi}]$, where $\bar{\phi}$ is the mean pressure head) and, therefore, Eqs. (56) and (57) lead to

$$\sigma_{q_1}^2 = \sigma_f^2 (K_g \exp[\alpha_g \bar{\phi}])^2 \left\{-\frac{5}{2}\frac{1}{\mu} + \frac{6}{\mu^2} + \frac{3}{\mu^3} - \frac{6}{\mu^4} + \ln(1+\mu)\left[\frac{2}{\mu} - \frac{8}{\mu^3} + \frac{6}{\mu^5}\right]\right\}, \tag{58}$$

$$\sigma_{q_2}^2 = \sigma_{q_3}^2 = \sigma_f^2 (K_g \exp[\alpha_g \bar{\phi}])^2 \left\{\frac{1}{4}\frac{1}{\mu} - \frac{1}{\mu^2} - \frac{3}{2}\frac{1}{\mu^3} + \frac{3}{\mu^4} + \ln(1+\mu)\left[\frac{2}{\mu^3} - \frac{3}{\mu^5}\right]\right\}, \tag{59}$$

which are identical to those found by Yeh et al. [21] using the unit mean head gradient assumption.

From Eqs. (56) and (57) the coefficients of variation of the specific discharge in the longitudinal and transverse directions are obtained, respectively, in the forms

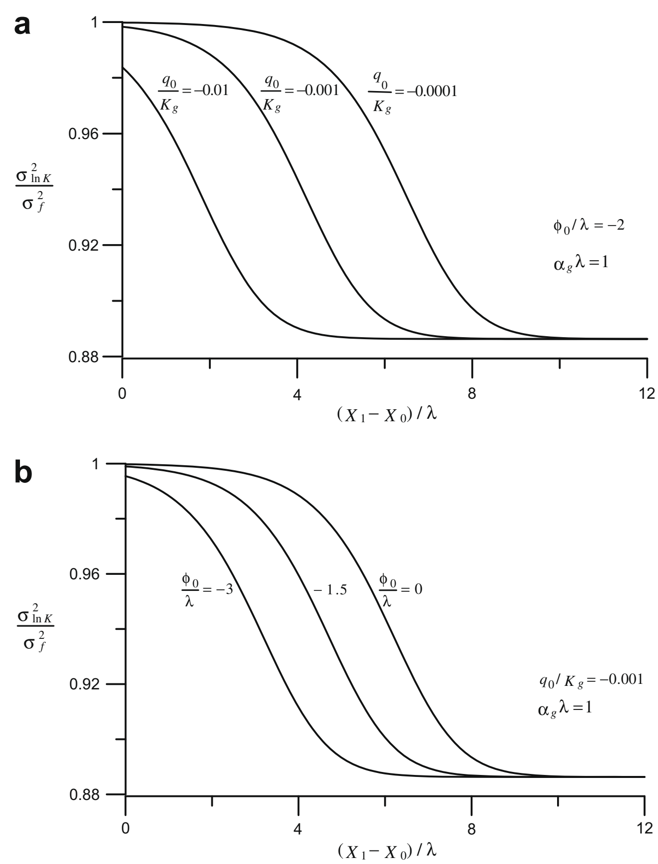

Fig. 2. Dimensionless variance of log unsaturated hydraulic conductivity versus dimensionless distance from the boundary of constant pressure head for various (a) infiltration rates and (b) prescribed pressure heads at the bottom boundary.

$$\frac{\sigma_{q_1}}{\langle q \rangle} = \sigma_f \sqrt{-\frac{5}{2}\frac{1}{\mu} + \frac{6}{\mu^2} + \frac{3}{\mu^3} - \frac{6}{\mu^4} + \ln(1+\mu)\left[\frac{2}{\mu} - \frac{8}{\mu^3} + \frac{6}{\mu^5}\right]}, \tag{60}$$

$$\frac{\sigma_{q_2}}{\langle q \rangle} = \frac{\sigma_{q_3}}{\langle q \rangle} = \sigma_f \sqrt{\frac{1}{4}\frac{1}{\mu} - \frac{1}{\mu^2} - \frac{3}{2}\frac{1}{\mu^3} + \frac{3}{\mu^4} + \ln(1+\mu)\left[\frac{2}{\mu^3} - \frac{3}{\mu^5}\right]}. \tag{61}$$

These results suggest that the boundary conditions have no influence on the variation (or dispersion) of the specific discharge, which are important in the analysis of solute transport, in the case of a constant soil pore-size distribution parameter. It is important to recognize that the influence of the boundary conditions is reflected in the behavior of mean pressure head. The mean flow and mean pressure head are directly related through the Darcy's law. In other words, the boundary conditions implicitly affect the behavior of mean flow. Therefore, the coefficient of variation of the specific discharge, which measures the variation in specific discharge relative to the mean discharge, is independent of the boundary conditions.

4. Comparison of the pressure head variance with the published result

It is of interest to justify the application of the nonstationary spectral approach to unsaturated flow problems involved in nonstationarity in the statistics of random velocity fields by comparing with the published results. Lu et al. [14] have developed a first-order analytical solution to the pressure head variance for one-dimensional (1-D) steady state unsaturated flow in randomly heterogeneous layered soil columns under various random boundary conditions. The comparison of our analytical expression for the pressure head variance with the result of Lu et al. [14] is presented below.

For the comparison, the boundary conditions are included in the evaluation of the pressure head variance in the 1-D case, which have been neglected in the 3-D case. To determine the pressure head variance, one needs to calculate σ^2_ε, which is determined from the transfer function given by Eq. (25). For the 1-D flow case, Eq. (25) is reduced to

$$\frac{d^2\Phi_f}{dX_1^2} + \alpha_g \frac{d\Phi_f}{dX_1} = i\frac{q_0}{K_g} R_1 \exp[iR_1X_1] \tag{62}$$

subject to the boundary conditions

$$\Phi_f = 0 \quad X_1 = X_o, \tag{63a}$$

$$\frac{d\Phi_f}{dX_1} + \alpha_g \Phi_f = \frac{q_0}{K_g}\exp[iR_1X_1] \quad X_1 = X_L, \tag{63b}$$

where Eqs. (63a) and (63b) are obtained by applying Eq. (24) into Eqs. (17a) and (17b), respectively. The solution of Eqs. (62) and (63) is given by

$$\Phi_f = i\frac{q_0}{K_g}\frac{1}{R - i\alpha_g}(-\exp[iRX_1] + \exp[iRX_0]\exp[-\alpha_g(X_1 - X_0]). \tag{64}$$

Substituting Eq. (64) into Eq. (24) yields

$$\varepsilon'(\boldsymbol{X}) = \frac{q_0}{K_g}\int_{-\infty}^{\infty}\frac{i}{R - i\alpha_g}(-\exp[iRX_1] + \exp[iRX_0] \times \exp[-\alpha_g(X_1 - X_0)])dZ_f(R). \tag{65}$$

The equation for σ^2_ε is obtained upon applying the representation theorem for ε' as follows:

$$\sigma^2_\varepsilon = \left(\frac{q_0}{K_g}\right)^2\left\{(1 + \exp[-2\alpha_g(X_1 - X_0)])\int_{-\infty}^{\infty}\frac{S_{ff}(R)}{R^2 + \alpha_g^2}dR - 2\exp[-\alpha_g(X_1 - X_0)]\int_{-\infty}^{\infty}\frac{\cos[R(X_1 - X_0)}{R^2 + \alpha_g^2}S_{ff}(R)dR\right\}. \tag{66}$$

With this result Eq. (66), the pressure head variance can be determined from Eq. (30).

We assume the same exponential form of the covariance function of $\ln K_s$ previously used by Lu et al. [14] in the determination of the pressure head variance in the case of 1-D unsaturated flow. The associated spectral density function with an exponential covariance function of $\ln K_s$ has the form

$$S_{ff}(R) = \frac{\sigma_f^2\lambda}{\pi(1 + \lambda^2R^2)}. \tag{67}$$

The σ^2_ε results from Eqs. (66) and (67) in the form

$$\sigma^2_\varepsilon = \left(\frac{q_0}{K_g}\right)^2\frac{\sigma_f^2\lambda^2}{\mu}\left\{(1 + \exp[-2\mu\xi])\frac{1}{1+\mu} - \frac{2}{1-\mu^2}(\exp[-2\mu\xi] - \mu\exp[-(1+\mu)\xi])\right\}, \tag{68}$$

where $\mu = \alpha_g\lambda$ and $\xi = (X_1 - X_0)/\lambda$. The pressure head variance in Eq. (30) with a constant α is given now by

$$\sigma^2_\phi = \left(\frac{q_0}{K_g}\right)^2\frac{\sigma_f^2\lambda^2}{\rho^2\mu}\left\{(1 + \exp[-2\mu\xi])\frac{1}{1+\mu} - \frac{2}{1-\mu^2}(\exp[-2\mu\xi] - \mu\exp[-(1+\mu)\xi])\right\}, \tag{69}$$

where $\rho = \alpha_g\bar{\varepsilon} = \exp[\mu(\phi_0/\lambda - \xi)] + (q_0/K_g)(\exp[-\mu\xi] - 1)$. This is identical to the result of Lu et al. [14] (their Eq. (21)) with a constant α under deterministic boundary conditions.

5. Conclusions

A spectral approach based on Fourier–Stieltjes representations for the perturbed quantities has been applied to the case of the quantification of field-scale flow processes in a partially saturated heterogeneous porous medium. The flow domain is assumed to be in a formation of infinite horizontal extent, bounded above by a constant flux at the surface and below by a prescribed pressure head at a certain depth below the soil surface. The general expressions for the pressure head variance, variance of log unsaturated hydraulic conductivity and variance of the specific discharge are presented in the wave number domain. The closed-form expressions are developed for the simplified case of statistical isotropy of the log hydraulic conductivity field with a constant soil pore-size distribution parameter. The impact of the boundary conditions on these results is examined.

It was found that the variance of pressure head increases with the infiltration rate. This is attributed to the influence of the pore-scale variability on the pressure head variability which is more persistent for a larger infiltration rate. As expected, the higher the constant pressure head (more negative) at the boundary, the higher the variability of pressure head for a given infiltration rate. A larger infiltration rate or a higher constant pressure head at the boundary leads to a reduction in variance of unsaturated $\log K$. The boundary conditions have no influence on the variation of longitudinal and transverse specific discharge in the case of a constant soil pore-size distribution parameter. The result for the pressure head variance, obtained by applying the nonstationary spectral approach to 1-D unsaturated flow field, is identical to the published result in Lu et al. [14].

Acknowledgements

Research leading to this work has been partially supported by the grants from Taiwan National Science Council under the contract number NSC 96-2221-E-009-087-MY3. We are grateful to the four anonymous reviewers for constructive comments that improved the quality of the work.

References

[1] Bakr AA, Gelhar LW, Gutjahr AL, MacMillan JR. Stochastic analysis of spatial variability in subsurface flows: 1. Comparison of one- and three-dimensional flows. Water Resour Res 1978;14(2):263–71.
[2] Bear J. Dynamics of fluids in porous media. New York: Dover; 1972.
[3] Chang C-M, Yeh H-D. Large-time behavior of macrodispersion in heterogeneous trending aquifers. Water Resour Res 2007:W11501. doi:10.1029/2007WR006017.
[4] Chang C-M, Yeh H-D. Using the nonstationary spectral method to analyze asymptotic macrodispersion in uniformly recharged heterogeneous aquifers. J Hydrol 2008. doi:10.1016/j.jhydrol.2007.12.006.
[5] Ferrante M, Brunone B, Yeh T-C. Uncertainty analysis of transient unsaturated flow in bounded domain. Water Resour Res 2002;38(2). doi:10.1029/2001WR001015.
[6] Gardner WR. Some steady state solutions of unsaturated moisture flow equations with application to evaporation from a water table. Soil Sci 1958;85(4):228–32.
[7] Gelhar LW, Axness CL. Three-dimensional stochastic analysis of macrodispersion in aquifers. Water Resour Res 1983;19(1):161–80.
[8] Harter T, Zhang D. Water flow and solute spreading in heterogeneous soils with spatially variable water content. Water Resour Res 1999;35(2):415–26.
[9] Indelman P, Or D, Rubin Y. Stochastic analysis of unsaturated steady state flow through bounded heterogeneous formations. Water Resour Res 1993;29(4):1141–8.
[10] Li S-G, McLaughlin D. A nonstationary spectral method for solving stochastic groundwater problems: Unconditional analysis. Water Resour Res 1991;27(7):1589–605.
[11] Li S-G, McLaughlin D. Using the nonstationary spectral method to analyze flow through heterogeneous trending media. Water Resour Res 1995;31(3):541–51.
[12] Lu G, Zhang D. Nonstationary stochastic analysis of flow in a heterogeneous semiconfined aquifer. Water Resour Res 2002;38(5). doi:10.1029/2001WR000546.
[13] Lu Z, Zhang D. Analytical solutions to steady state unsaturated flow in layered, randomly heterogeneous soils via Kirchhoff transformation. Adv Water Resour 2004;27:775–84.
[14] Lu Z, Zhang D, Robinson BA. Explicit analytical solutions for one-dimensional steady state flow in layered, heterogeneous unsaturated soils under random boundary conditions. Water Resour Res 2007:W09413. doi:10.1029/2005WR004795.
[15] Mantoglou A, Gelhar LW. Stochastic modeling of large-scale transient unsaturated flow systems. Water Resour Res 1987;23(1):37–46.
[16] Russo D. Stochastic analysis of the velocity covariance and the displacement covariance tensors in partially saturated heterogeneous anisotropic porous formations. Water Resour Res 1995;31(7):1647–58.
[17] Russo D, Bouton M. Statistical analysis of spatial variability in unsaturated flow parameters. Water Resour Res 1992;28(7):1911–25.
[18] Russo D, Russo I, Laufer A. On the spatial variability of parameters of the unsaturated hydraulic conductivity. Water Resour Res 1997;33(5):947–56.
[19] Sun AY, Zhang D. Prediction of solute spreading during vertical infiltration in unsaturated, bounded heterogeneous porous media. Water Resour Res 2000;36(3):715–23.
[20] Tartakovsky DM, Neuman SP, Lu Z. Conditional stochastic averaging of steady state unsaturated flow by means of Kirchhoff transformation. Water Resour Res 1999;35(3):731–45.
[21] Yeh T-C, Gelhar JW, Gutjahr AL. Stochastic analysis of unsaturated flow in heterogeneous soils, 1. Statistically isotropic media. Water Resour Res 1985;21(4):447–56.
[22] Zhang D, Winter CL. Nonstationary stochastic analysis of steady state flow through variably saturated, heterogeneous media. Water Resour Res 1998;34(5):1091–100.